

Pulsed Nuclear Magnetic Resonance

Evan Berkowitz*

Junior, MIT Department of Physics

(Dated: November 22, 2006)

After an in-depth discussion about the history, potential, and theory of nuclear magnetic resonance, we measure the T_1 of 100% glycerine via two techniques, T_2 for many viscosities via the Carr-Purcell method, and the magnetic moment of hydrogen by determining its Larmor frequency.

1. HISTORY AND FUTURE POTENTIAL

Nuclear magnetic resonance (NMR) is a scientific principle which arises from the magnetic properties of an atom's nucleus. Both protons and neutrons have magnetic moments, meaning that they interact in certain ways with magnetic fields. In 1952, Felix Bloch and Edward Mills Purcell won the Nobel Prize "for their development of new methods of nuclear magnetic precision measurements and discoveries in connection therewith." [1] Since its discovery, it has revolutionized many areas of science and has had a large impact on everyday life.

The two laureates developed methods for determining the magnetic moments of nuclei by measuring the frequencies of oscillating electromagnetic fields which gave insight into the transfer of energy between their samples and the measuring device. [2]

The theory behind NMR requires quantum physics, which emerged in the 1920s. Following the Stern-Gerlach experiment which demonstrated the two-state nature of spin, other similar experiments with much higher accuracy showed the existence of a discovered nuclear magnetic moment in an experiment similar to their famous electron-spin experiment with much higher precision.

In 1946 Bloch and Purcell independently discover NMR. During World War II Purcell had worked in the MIT Radiation Laboratory, which allowed him to become familiar with the creation and detection of high-frequency radiation as well as its absorption by matter. In all likelihood, his familiarity with this technology allowed him to probe further, discovering NMR. [3] At the beginning of the war, Bloch worked on atomic energy at Los Alamos National Laboratory but eventually also joined the effort to develop radar. [4]

Originally, NMR the main technique for exploring the NMR phenomenon was continuous wave (CW) spectroscopy. One method of CW spectroscopy required the magnetic field applied to the sample remain constant and the frequency of the applied oscillating field be broadly swept in order to determine the resonant areas of the spectrum. The other method of CW spectroscopy had the oscillating field held at a constant frequency and the magnetic field varied. Both methods allow the discovery

of the resonance conditions of the sample.

More recently, Fourier transform nmr (FT-NMR) has become more precedent. A Fourier Transform is a method of converting time domain data to the frequency domain or vice-versa. This ability allows many frequencies to be probed simultaneously. However, transforming the data is time intensive and difficult to do by hand, so this technique could only become generally useful once computers could take over the data analysis. FT-NMR's power was first shown by Ernst, who won a Nobel Prize in chemistry in 1991.

NMR has many practical uses. Most importantly, NMR provides the phenomenon behind the medical technique known as magnetic resonance imaging (MRI). MRI takes advantage of the fact that different substances in the body have different characteristics which can be obtained via NMR techniques. MRI allows doctors to peer inside of their patients without making an incision, making the discovery of abnormalities and their diagnosis much easier. Additionally, NMR has no effect on molecular electron structure, meaning that the patient's body chemistry is completely unaffected during the procedure. [5]

NMR has other uses as well. In biochemistry, it has begun to replace X-ray crystallography as the method of determining molecular structure. NMR spectroscopy can be used in the identification of compounds or isotopes, such as ^1H and ^{13}C . As we will see later, some aspects of NMR have particularly long timescales, so comparison across experiments can yield information about reactions which occur quickly. [3]

NMR has been used to construct basic quantum computers, which can solve problems much faster than classical computers. For instance, known algorithms for quantum computers can factor numbers much faster than any known algorithm for classical computers. In the last decade, rudimentary NMR-based quantum computers have been created and have shown their power. As a proof of concept, scientists configured the computer to factor 15 and received 5 and 3 as results. Though not particularly astonishing, this result shows the promise of the techniques required. Improvements in quantum computation has implications for areas such as cryptography and cryptanalysis, as well as search [6] As recently as this week a breakthrough has been announced in a letter to the journal Nature. Stegner et al. have discovered a technique for measuring spin quantum states in a purely electrical manner which will allow the read-

*Electronic address: evan_b@mit.edu

ing of quantum-processed data into familiar electronic computers.[7]

2. THEORY

NMR can be understood as a macroscopic culmination of microscopic phenomena. The root of NMR is the general two-state system, a solved problem in quantum mechanics. The Hamiltonian of such a problem is well understood and can be solved easily by a change of coordinates into a rotating frame, whose angular velocity is matched to the rate of precession of a magnetic moment in an appropriate field. Classically, the energy of a magnetic moment is given by

$$E = -\vec{\mu} \cdot \vec{B} \quad (1)$$

where $\vec{\mu}$ is the magnetic moment and \vec{B} is the magnetic field. With γ representing the gyromagnetic ratio and B_0 the z -component of the magnetic field, the frequency with which we can rotate a vertical moment through the xy -plane and back to its vertical orientation is given by

$$\omega_0 = \gamma B_0 \quad (2)$$

This frequency is known as the Larmor frequency, which can be thought of as the frequency which corresponds to the energy difference between the spin-up state $|\uparrow\rangle$ and the spin-down state $|\downarrow\rangle$. Only when the rotating portion of the applied field is near the Larmor frequency can a $|\uparrow\rangle$ be rotated away from the $+z$ -axis.[5]

When dealing with a reasonable sample, the number of particles subject to this phenomenon is large. If there are millions of particles in our then the microscopic view begins to disappear and we can speak of the macroscopic *net* magnetic moment. A sample we might examine would have on the order of 10^{23} particles, meaning that we can treat the entire net magnetic moment as an ensemble of continuously variable macroscopic moments, each itself comprised of millions of quantized moments. Conveniently, its quantized parts give the net moments have the same Larmor frequencies.

Once the rotation of a moment away from the $+z$ -axis by a rotating field near the Larmor frequency is understood, the repercussions of such a rotation must be investigated. Since the angular velocity with which the moment is rotated away from the $+z$ -axis is constant, we can correlate a time with an angle by figuring out multiplying by this rate.

There are three major effects which govern the spin vector's evolution. The first is the spin-lattice relaxation of the ensemble. Since entropy would prevent all the states from being $|\uparrow\rangle$ even in the presence of a magnetic field, there is some equilibrium which would be reached in the long run. Therefore, spin-lattice relaxations are understood to be cooling phenomena, with the entire moment coming to equilibrium with its environment. The time constant T_1 describes the time it

takes the z -magnetic moment to recover $1 - \frac{1}{e}$ from a 180° rotation.

The second interaction is the spin-spin relaxation, which can be best understood as the interaction between two ensembles' spin vectors. By breaking the sample into ensembles as small as millions of particles, the net spin vectors can interact in a complicated manner. The time constant T_2 is the time it takes for the projection of the spin vector onto the xy -plane to shrink by a factor of e .

The third effect is the inhomogeneity of the magnetic field. If two ensembles are subject to fields of different strength then their precession frequency will also be different, meaning that they will become out of phase as time passes. Hence, the net spin from their combination will shrink with time even though the spin of no particular ensemble is weakening. The time constant T_2^* describes this effect and depends on T_2 . It can be shown[2] that if ΔH is the field difference then

$$\frac{1}{T_2^*} = \frac{1}{T_2} + \gamma \Delta H \quad (3)$$

When one sees free induction decay (FID), the response which is measured from this effect, the oscillations are contained in an envelope decaying like T_2^* .

Since we can measure changing magnetic fields, and the moment is precessing about the $+z$ -axis, two pulses are of particular interest to us. The first is a 90° pulse, which would give the rotate the vector into the xy -plane, meaning the largest portion of the vector would be rotating and yielding the largest FID. The second is a 180° pulse, which would rotate the vector to the $-z$ -axis, meaning that no portion of the vector would be rotating, and that we should see no FID. However, if the vector was already in the xy -plane before the 180° pulse, it would remain the the plane afterwards.

180° pulses applied to vectors in the xy -plane give rise to a feature of an NMR response called the spin echo. If the ensembles are all $|\uparrow\rangle$, and a 90° pulse is applied, they will all be in the xy -plane, in phase. Due to local differences in the magnetic field, they will precess with different rates, becoming out of phase. Once a 180° pulse is applied, the spins which rotated more quickly are now behind those that precessed more slowly, and can catch up. meaning that the spins will return to being in phase in a time equal to the time difference between the 90° and 180° pulse.

3. EXPERIMENTAL APPARATUS

Our apparatus was constructed in a way that we could easily change what we were examining. There were two large permanent magnet, generating a field of 1764 ± 3 gauss, between which we could place a small test tube with a sample. The magnetic field was measured with a gaussmeter which was calibrated against a zero-gauss chamber and a magnet with a field strength of 2004 gauss

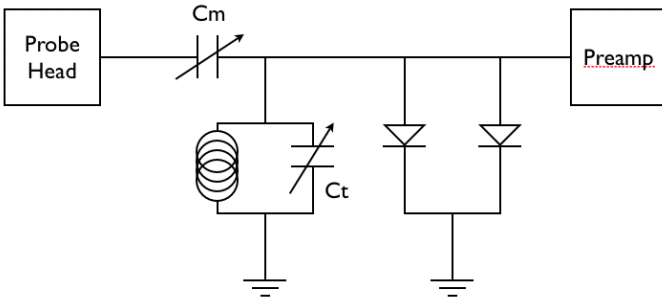


FIG. 1: A circuit diagram of the probe. The probe head supplies the location in which the magnetic field can induce a signal in our circuit.

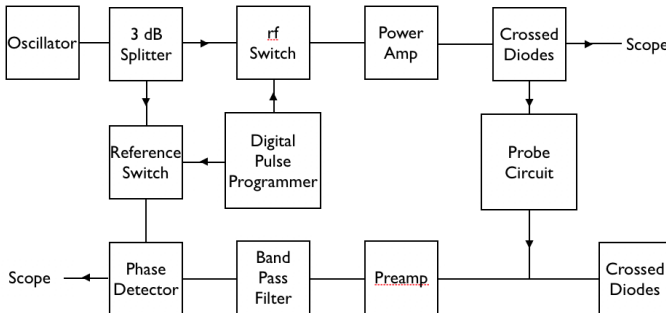


FIG. 2: The experimental apparatus which allowed us flexibility in which experiments we performed.

$\pm 5\%$. With 5 measurements, we determined that the calibration magnet had a field strength of 2002 ± 2.7 gauss, which is well within error. In six measurements, we found the magnet in our apparatus to have a strength of 1763 ± 3 gauss.

The probe was connected to the the pulse-generation circuitry, which consisted primarily of an oscilloscope for measurements, an oscillator, responsible for producing sinusoidal signal, a digital pulse programmer, which allowed us to program how many pulses to send, how long they should last, and the separation between them. The programmer also allowed us to run one trial after the next with a repeat time of our choosing. In order to avoid interference between trials, we tried to set the repeat time to approximately five times the decay time. The probe itself consisted of a probehead, which would have a current induced in it by the rotating magnetic field, an inductor and variable capacitors which allowed us to tune our probe circuit for maximal response on each sample. The probe can be seen in figure 1, and exactly how it fits into our circuit as a whole can be seen in figure 2.

4. THE MAGNETIC MOMENT OF HYDROGEN

To measure the magnetic moment of hydrogen, one must dig deeper into (2). It turns out that γ is actually

the product of a variety of constants, resolving to

$$\gamma = \frac{\mu}{\hbar I} \quad (4)$$

where μ is the magnetic moment of hydrogen, \hbar is Planck's reduced constant, and I is the spin angular momentum.[2] Then, we can solve the relationship given in (2) to be a formula for mu , as a ratio of ω_0 and B_0 . After calibrating the gaussmeter and measuring the magnetic field as described in Section 3, we attempted to find the resonant frequency by capturing as much area under the response curve as possible, without an oscillation. By performing repetitive measurements, we found that the resonant frequency was 7.526 ± 0.001 MHz. Theory would predict that with a magnetic field of 1764 ± 3 gauss, we would measure a resonant frequency of 7.51 ± 0.014 MHz. Our experimental value was only a small fraction greater than one σ away from the predicted value.

5. T_1 DECAY TIME

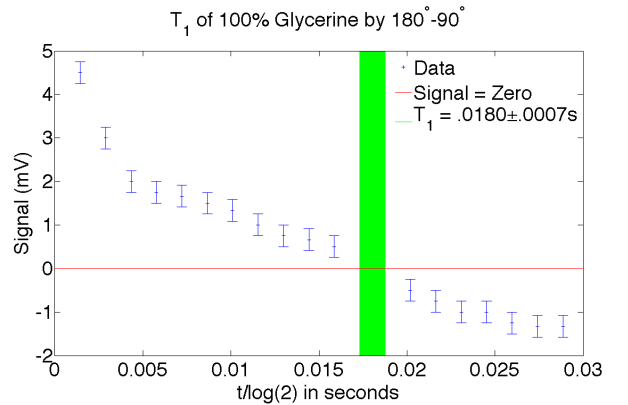


FIG. 3: A plot of the system's response to waiting t between the two pulses. The green range on the was obtained through a linear interpolation of the points near the lack of data. Data is missing because as the signal passes close to zero, it is dominated by the noise in the signal. We found that any signal less than approximately .4 mV were impossible to distinguish from noise.

T_1 may be measured through both the 90° - 90° and the 180° - 90° pulse sequence. The 90° - 90° sequence first rotates the spin vector into the xy -plane, and after some time the z -component has recovered some amount. By adding another, we rotate the vectors in the xy -plane into the z -axis, removing the response from that population while simultaneously we change the recovered z -component into the xy -plane, meaning that the visible response is proportional to the amount recovered. The 180° - 90° sequence first flips the moment to be on the $-z$ -axis. After the population relaxes for a time, a 90° pulse is applied, revealing the recovered z -component. Since T_1 represents a 63% recovery, we can also calculate that

a 50% recovery (ie. the vector is in the xy -plane) corresponds to the time $T_1 \cdot \ln(2)$. So, by waiting $T_1 \cdot \ln(2)$ before the second pulse, the result will be vectors on the z -axis, meaning no response will be seen.

The 180° - 90° sequence data for 100% glycerin can be seen in Figure 3. By the 180° - 90° sequence, we measured T_1 to be 18 ± 0.7 ms. By the 90° - 90° sequence, we measured T_1 to be 20.2 ± 1.9 ms. These two values are close, and give us a good range for the true value of T_1 of 100% glycerin.

6. T_2 DECAY TIME

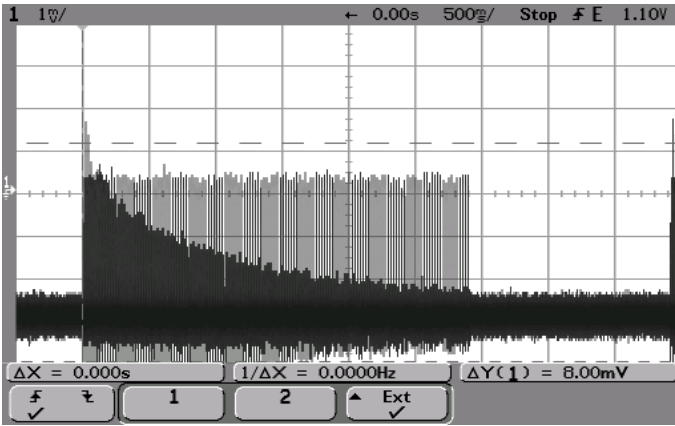


FIG. 4: With a short τ and a high N (180° pulses in the sequence), one can view the decay of the magnitude of the xy -plane component of the spin vector.

T_2 can be measured by a Carr-Purcell sequence, which is best described as 90° - τ - 180° - 2τ - 180° - 2τ - 180° - 2τ ... which would generate spin echoes at time 2τ , 4τ , 6τ , 8τ ... by essentially extending the idea behind the 90° - 180° pulse as explained in Section 2. By having a small τ and a large number of applied pulses, one can generate a curve like the one shown in Figure 4. Over many trials of measuring the time it took to decay by a factor of e , we determined the T_2 value of 100% glycerin to be 15.9 ± 0.6 ms.

7. VISCOSITY

In order to measure the trend of T_1 and T_2 across viscosities, we used samples of water-glycerin solutions. By weight, the solutions were 100% glycerine, 80%, 60%, 40%, 20% and water bubbled with N_2 to remove the paramagnetic O_2 . The data accumulated can be seen in Figure 5. Using a linear fit on the log of both the viscosity dataset and the decay-time data set, we found the fits described in the figure.

The success of the Carr-Purcell method relies on the fact that the moments create fields the other moments

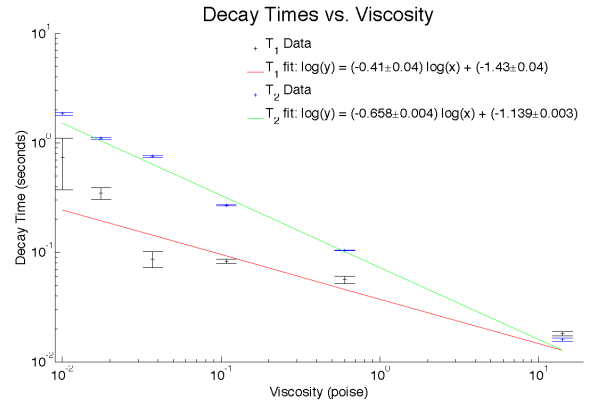


FIG. 5: T_1 and T_2 data for various water-glycerin solutions. Only the most viscous data point has $T_1 < T_2$

nearby can relax through the spin-spin interactions. In order for the ensembles to have enough time to interact and equilibrate, the mixing rate in the sample should be low. So, for viscous liquids, T_2 should be short because mixing is least, and shorter than T_1 for viscous liquids whose fluctuations have large low-frequency components.[2]

In theory, T_1 should always be at least T_2 , but for all but the most viscous data point we found that T_1 was actually less than T_2 . Since T_2 was very easy to measure, but T_1 was measured with the 180° - 90° sequence, which is dominated by noise in the range in which you are trying to find no response, we can conclude that the 180° - 90° pulse sequence is insufficient for measuring T_1 for glycerin solutions.

Alone, the T_2 data matches Bloembergen's data fairly well.[8] The data is on the same scale, and displays approximately the same relationship in terms of the slope on the log-log plot. This confirms, to some extent, the accuracy of our T_2 measurements.

8. ERROR

Error arises in these data from various sources. Among the more prominent sources was the fact that in order to see any results, you cannot use resonance conditions but must be off resonance. The variable capacitor in the probe circuit was another source of error because it needed to be tuned to each different kind of substance that was being probed in order to get the maximal response. Since the capacitor was continuously variable, it is unlikely that it was ever set to exactly the same setting from one day to the next, making it difficult to compare the error. Frustratingly, the entire NMR setup is touch-sensitive and the oscilloscope readings are significantly different when one even lightly touched the frame. Moreover, the location of the vial was not set permanently, and on a few occasions moved from being the apparatus being bumped between samples. Due to the quick repeat times,

it was sometimes hard to gauge the height of the decay and correlate a decay time for it. NMR experiments are also notoriously bad for their signal-to-noise ratio, which is usually low.[3]

For the viscosity data set, the first additional source of error is the solutions themselves. The solutions were prepared by weight, which can be error-prone and none of the solutions are necessarily the percentages they claim. Another source is temperature fluctuations and the fact that the viscosity lookup table did not have room-temperature data.

we had a difficult time adapting to the apparatus and understanding what was going on. In spite of difficulties we did manage to measure the magnetic moment of hydrogen through its Larmor frequency. We were able to observe FIDs and the Carr-Purcell phenomenon. While our $180^\circ\text{-}90^\circ T_1$ data is unreliable, our T_2 looks very good when compared with Bloembergen's data. Finally, the two different methods of measuring T_1 for only 100% glycerin seemed reliable as we arrived at nearly the same time for two entirely different methods.

9. CONCLUSIONS

Due to the many sources of error, the experiment was at times very frustrating to perform. In the beginning,

-
- [1] *The Nobel Prize in Physics 1952* (2006), URL http://nobelprize.org/nobel_prizes/physics/laureates/1952/.
 - [2] MIT Department of Physics, *Pulsed Nuclear Magnetic Resonance: Spin Echoes*, JLExp12.pdf (2006).
 - [3] W. Authors, *Nuclear Magnetic Resonance* (2006), URL http://en.wikipedia.org/wiki/Nuclear_magnetic_resonance.
 - [4] W. Authors, *Felix Bloch* (2006), URL http://en.wikipedia.org/wiki/Felix_Bloch.
 - [5] K. Rajogopal, *The General Two-State Problem* (2006).
 - [6] S. Lloyd and P. Penfield, *6.050 Lecture - Quantum Computing* (2005).
 - [7] A. R. S. et al., *Electrical detection of coherent ^{31}P spin quantum states* (2006), URL <http://www.nature.com/nphys/journal/vaop/ncurrent/full/nphys4%65.html>.
 - [8] N. Bloembergen, *Nuclear Magnetic Resonance, A Reprint Volume* (W. A. Benjamin, Inc, 1961).